THE BALTIC JOURNAL
OF ROAD AND BRIDGE ENGINEERING

2011
6(3): 193–200

CALCULATION MODEL FOR STEEL FIBRE REINFORCED CONCRETE PUNCHING ZONES OF BRIDGE SUPERSTRUCTURE AND FOUNDATION SLABS

Gediminas Marčiukaitis[1], Remigijus Šalna[2] ✉, Bronius Jonaitis[3], Juozas Valivonis[4]

Dept of Reinforced Concrete and Masonry Structures, Vilnius Gediminas Technical University, Saulėtekio al. 11, 10223 Vilnius, Lithuania
E-mails: [1]gelz@vgtu.lt; [2]remigijus.salna@vgtu.lt; [3]bronius.jonaitis@vgtu.lt; [4]juozas.valivonis@vgtu.lt

Abstract. The usage of steel fibre reinforced concrete in monolithic joins is well known as a good alternative of additional reinforcement because of chaotic distribution of steel fibres in complex stress ant strain state. Unfortunately, the analysis of well known design codes and different models even in punching case without steel fibres shows that there is no common theory in calculating punching shear strength. Existing models of punching shear strength with steel fibres are mainly based on empirical coefficients, or require direct tests, what makes the design of such structures more complicated. Besides, the analysis of elastic and plastic characteristics of steel fibre reinforced concrete is incomplete, because there is no unified, well-grounded theory to evaluate them. The aim of this paper is to present steel fibre reinforced concrete punching shear strength model. Suggested steel fibres reinforced concrete punching shear strength model estimates the main factors, such as concrete strength, longitudinal reinforcement, steel fibres volume, type, geometric and anchoring characteristics, and also plastic strains of steel fibre reinforced concrete. The comparison of suggested model with tests results demonstrates good accuracy of the suggested model for steel fibre reinforced concrete slabs (mean value – 1.12, standard deviation – 0.08 coefficient of variation – 7%).

Keywords: punching shear strength, steel fibres, reinforced concrete, plastic strains, complex stress and strain state.

1. Introduction

In many cases complicated stress and strain state due to load action in structures of bridges appears. That is the case with joints between flat slabs and columns, columns to foundations joints, connections of columns to piles, etc. The said and other structural bridge members may be subjected to impulse and cycle loads. Various types of stresses in these areas of structures are generated: compression, tension, local compression, shear etc. It is well known that the highest strength of the concrete is in compression and the lowest – in tension. When strengthening of a concrete zone subjected to the action of forces in one direction only is required then one direction reinforcing is applied. But in the case of complicated stress state reinforcing by bars becomes either complicated or even economically unjustifiable. Such state of stress takes place in some bridge structures, e. g. in superstructure decks supported on columns and these – on foundation reinforced concrete (RC) slab (Fig. 1). For such structures or its elements more effective materials are materials with higher mechanical and deformation properties in all directions of axis. Such material for many RC structures is steel fibre reinforced concrete (SFRC) (Baikovs, Rocēns 2010; Szmigiera 2007; Šalna, Marčiukaitis 2007).

Analytical models and mechanical calculation methods for SFRC were created. Compression and tension strengths and elasticity modulus of SFRC were most widely investigated. They are the main properties that allowed starting using such type of concrete for load bearing RC structures or their parts. In some countries standards and technical recommendations regulating quality and requirements for SFRC products are established: in the USA – *ASTM C1018-97 Standard Test Method for Flexural Toughness and First-Crack Strength of Fiber-Reinforced Concrete (Using Beam with Third-Point Loading),* in Japan – *JSCE-SF4: 1984. Method of Tests for Flexural Strength and Flexural Toughness of Steel Fibre Reinforced Concrete,* in the United Kingdom – *TR34 Report (1995), General document and Appendix F: Slab Design with Steel Fibres*, in Russia – *СП 52-104-2006: Сталефибрбетонные Конструкции* [SP 52-104-2006: Steel Fibre Reinforced Concrete Structures], etc.

Nevertheless, methods for determination of properties and estimation, values of results according to the said

ISSN 1822-427X print / ISSN 1822-4288 online
doi: 10.3846/bjrbe.2011.25
http://www.bjrbe.vgtu.lt

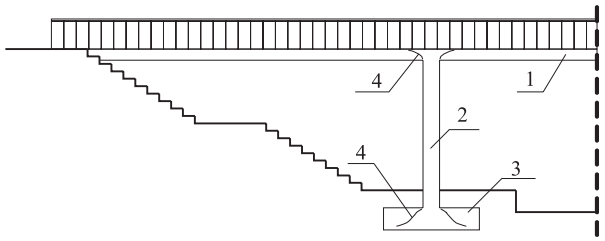

Fig. 1. Diagram of a bridge with superstructure and foundation RC slabs: 1 – superstructure deck slab; 2 – support (column); 3 – supporting foundation – slab; 4 – punching sections

documents differ in many cases; valuation of indices describing intermediate strength as well as rates relating strength and strain are assessed in different way. Generally, stress to strain, especially plastic ones, relation is determined by tests. There is a lack of theoretical and experimental investigations in behaviour of SFRC in elastic plastic stage. It is an obstacle in selecting a suitable model for punching strength analysis of SFRC slabs, e. g. in standards of *ASTM C1018-97* and *JSCE-SF4: 1984* accomplishment of experiments is proposed for determination of the actual σ-ε diagrams.

Investigation in punching strength analysis methods and in design codes of various countries (Šalna *et al.* 2004) pointed out that the opinion about punching strength analysis varies. According to the all said codes conditional tangential stress (τ_c) acting in a conditional critical area is conditionally described and does not reflect actual behaviour of structure at all. Moreover, effect of such important factor as the longitudinal reinforcement is taken in to account not in all codes. Influence of transverse reinforcement is evaluated not in the same way as well. Values of partial safety factors to the strengths of materials and to the loads as well are different.

There is no unified opinion about design for punching strength according to the all codes and there is no unified model for punching strength analysis as well. For description of models various theories were applied – theory of plasticity, of built-up bars, of failure etc. but the unified opinion was not reached. Analysis of models performed by Georgopoulos (1989), Broms (1990), Hallgren (1996), Menétrey (2002), Theodorakopoulos and Swamy (2002) also points out that in all models considered different design diagrams and different criteria are assumed. The principle stresses are related to the concrete strength characteristics in different way. It shows that punching is not sufficiently investigated and additional experimental and theoretical research is required.

Performed analysis of models makes it possible to distinguish the 2 model types:

I type – failure takes place due to shearing the compression zone by the principle stress (Broms 1990; Halgren 1998; Theodorakopoulos, Swamy 2002);

II type – failure takes place due to tension stress in diagonal section (Georgopoulos 1989, Menétrey 2002).

Presented review makes it clear that the models referred to the 2nd group are less realistic. Models referred to the 1st group reflect the real failure mode much better.

Most authors punching phenomenon consider as a plane problem, i.e. the same principles as for the strength of diagonal section for RC beam without shear reinforcement are applied. Then normal and diagonal cracks with the action of the principle stresses progress towards the compression zone and failure occurs when the compression zone is destructed under a certain combination of compression and shear stresses. Actually, the compression zone is under the action of tri-axial stress state but most authors neglect it. It is neglected in almost all design codes and recommendations.

Steel fibres in punching slab zone not only change interrelation between stresses of different types but also their distribution due to the influence of difference in strain properties and their character in elastic plastic structure behaviour stage. Thus, it is important to create such analytical model that would allow complete evaluation influence of steel fibres in determination of punching strength for RC superstructure deck slabs and foundations of bridge.

2. Diagram of analytical model and assumptions

Analytical model selected on the basis of investigation in strength and deformation properties of SFRC (Šalna, Marčiukaitis 2007) and behaviour of common slabs under punching (Broms 1990; Halgren, 1998; Theodorakopoulos, Swamy 2002) and according to general principles of mechanics is shown in Fig. 2.

For creation, analysis and investigation of the model the following assumption were made:

1) tension and compression stress strain diagrams for the materials are of trapezium shape (Fig. 3);
2) hypothesis of plain sections is valid;
3) in determination of the neutral axis location at failure the ultimate values of concrete strain are used;
4) diagram of normal stress in the compression zone – trapezium, that for tangential stress – in relationship with the normal stress;
5) failure occurs when compression zone of the slab is cut by the principle stress at an angle coinciding to the direction of the said stress.

Trapezoidal normal stress diagram is taken for determination of the compression zone. Investigations performed by different authors (Maalej, Li 1994) point out that application of trapezoidal σ-ε diagrams in compression and tension zones for SFRC gives results that show better

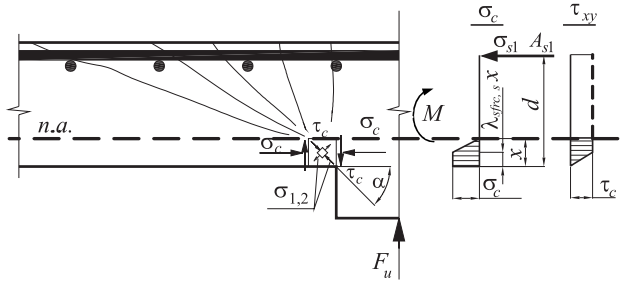

Fig. 2. Diagram of analytical model for punching

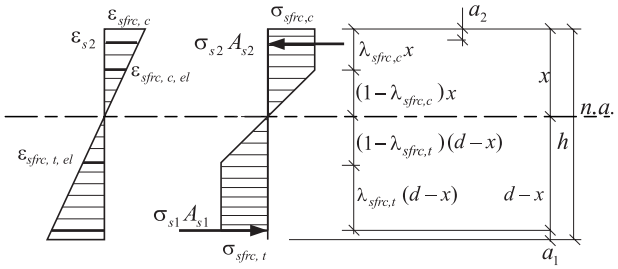

Fig. 3. Strain and stress diagrams in normal section of SFRC slab with allowance for plastic strain of concrete in tension and in compression

agreement with experimental ones than in the cases when rectangular or triangular diagrams are applied. Such diagrams are provided also in EC2.

Diagram for determination of neutral axis location for SFRC member is shown in Fig. 3. Stress diagrams for compression and tension zones assumed trapezoidal where elastic tension and compression fibre-concrete strains $\varepsilon_{sfrc,t,el}$, $\varepsilon_{sfrc,c,el}$ correspond to variable stress parts are represented by $\nu_{sfrc,t}(d-x)=(1-\lambda_{sfrc,t})(d-x)$ and $\nu_{sfrc,c}x=(1-\lambda_{sfrc,c})x$, while constant ones – correspondingly by $\lambda_{sfrc,c}(d-x)$ and $\lambda_{sfrc,c}x$. Here ν_{sfrc} and λ_{sfrc} – elasticity and plasticity coefficients for fibre-concrete.

λ_{sfrc} in tension and in compression are determined by empirical formulas obtained using results of experimental investigations. When steel fibres are with bends:

$$\left.\begin{aligned}\lambda_{sfrc,t}&=\lambda_t(2.06-0.015V_f^{1.5})\\ \lambda_{sfrc,c}&=\lambda_c(1+0.008V_f^{1.5})\end{aligned}\right\}, \tag{1}$$

where λ_c and λ_t – plasticity coefficients for concrete in compression and tension. According to investigations $\lambda_c=\lambda_t=1-0.061f_c^{0.5}$, since it is assumed that concrete elasticity module in tension and compression are equal.

Ratios between the average stress value and the max one in the diagrams, below referred to as stress diagrams completeness coefficients:

$$\left.\begin{aligned}\omega_{sfrc,t}&=\frac{1+\lambda_{sfrc,t}}{2}\\ \omega_{sfrc,c}&=\frac{1+\lambda_{sfrc,c}}{2}\end{aligned}\right\}. \tag{2}$$

Stresses in compression and tension zones corresponding to $\varepsilon_{sfrc,c}$ and $\varepsilon_{sfrc,t}$ strains related to tension reinforcement stress σ_{s_1}:

$$\left.\begin{aligned}\sigma_{sfrc,c}&=\sigma_{s1}\frac{1}{n_{sfrc,sc}}\frac{x}{d-x}\\ \sigma_{sfrc,t}&=\sigma_{s1}\frac{1}{n_{sfrc,st}}\end{aligned}\right\}, \tag{3}$$

where

$$\left.\begin{aligned}n_{sfrc,sc}&=\frac{E_{s1}}{E'_{sfrc,c}}=\frac{E_{s1}}{E_{sfrc,c}(1-\lambda_{sfrc,c})}\\ n_{sfrc,st}&=\frac{E_{s1}}{E'_{sfrc,t}}\frac{E_{s1}}{E_{sfrc,t}(1-\lambda_{sfrc,t})}\end{aligned}\right\}. \tag{4}$$

Then resultants acting in tension and compression of SFRC member are:

$$\left.\begin{aligned}&\omega_{sfrc,c}x\sigma_{sfrc,c}=\frac{1+\lambda_{sfrc,c}}{2n_{sfrc,sc}}\frac{x^2d}{d-x}\sigma_{s1}\\ &\sigma_{s1}A_{s1}\\ &\sigma_{s2}A_{s2}=\sigma_{s1}\frac{1}{n_{ss}}\frac{x-a_2}{d-x}A_{s2}\\ &\omega_{sfrc,t}(d-x)\sigma_{sfrc,t}=\omega_{sfrc,t}\frac{1}{n_{sfrc,st}}(d-x)\sigma_{s1}\end{aligned}\right\}. \tag{5}$$

When stresses and coefficients of their diagrams for the fibre-concrete are known it is simple to determine their resultants and to calculate compression zone depth from conditions of equilibrium for these resultants.

3. Analysis of normal and tangential stress diagrams in the compression zone

Analysis of publications revealed that different normal and tangential stress diagrams for principle stress calculations are used by the most of authors (Fig. 2). For example, Choi *el al.* (2007) apply cubic parabola for normal stress and for tangential one – trapezium, Shertwood *et al.* (2007) – trapezium for normal stress and square parabola – for tangential one, Zink (1999) – triangle for normal stress and cubic parabola – for tangential one. Nevertheless, trajectories of the principle stress depend very much on selected stress diagrams. Angle of the principle stress trajectory variation in relation to various selected combinations of normal and tangential stress diagrams is presented in the Table 1. When for normal stress trapezoidal diagram in relation to concrete plasticity coefficient (its completeness coefficient ω_σ = 0.8–1) and for tangential either trapezoidal or triangle diagrams (ω_σ = 0.5–1) are assumed, the results apparently differ. Between extreme completeness coefficient values, angle of the principle stress trajectory vary from α = 23 up to α = 57.

However, analysis of results of experimental investigations performed by Choi *et al.* (2007), Shertwood *et al.* (2007), Sharma (1986), Tuchlinski (2004) and Zink (1999) revealed that completeness coefficient for tangential stress diagram on average ω_τ = 0.65–0.75, which corresponds to the smaller spread of the principle stress trajectories angle: 33 –45. These values are commonly applied in classical theories and they generally agree with the experimental investigations of the said authors. Relation of these results with obtained experimental results and with idealized nor-

mal stress diagram expressed via plasticity coefficient gives completeness coefficients for normal and tangential stress diagrams:

$$\left.\begin{aligned}\omega_\sigma &= \frac{1+\lambda_c}{2}\\ \omega_\tau &= 0.43(1+\lambda_c)\end{aligned}\right\}. \quad (6)$$

Tangential stress diagram coefficient value determined in such way by formula varies within the limits of ω_τ = 0.6–0.75. It conforms to the completeness coefficient for diagrams described by square and cubic parabolas.

4. Principle stress and area of its action in the compression zone

According to proposed punching diagram presented in the Fig. 2 the principle stress depends on normal and shear (i.e. tangential) stresses.

Following the rule that the ultimate compression stress σ_u equals to the concrete compression strength f_c and the ultimate shear (tangential) stress at compression $\tau_u = 0.5f_c$, applying classical strength of materials formulas principle stress and angle its trajectory is expressed by:

$$\left.\begin{aligned}\sigma_{1,2} &= -\frac{\sigma_u}{2} \pm \sqrt{\frac{\sigma_u^2}{4} + \tau_u^2}\\ \tan 2\alpha &= \frac{2\tau_u}{\sigma_u}\end{aligned}\right\}. \quad (7)$$

Diagrams for determination of principle stress action in the compression zone area are given in Fig. 4.

When base and slant altitude of lateral surface for truncated pyramid and generatrix of lateral surface for truncated cone are expressed via x and α area of principle stress action in the compression zone may be determined using simple geometrical formulas:

$$\text{for circular columns } A = 4\left[(a + x\cot\alpha)\frac{x}{\sin\alpha}\right], \quad (8)$$

$$\text{for square columns } A = \pi\left[(a + x\cot\alpha)\frac{x}{\sin\alpha}\right], \quad (9)$$

where a – cross-sectional dimension of square column or cross-sectional diameter of circular column.

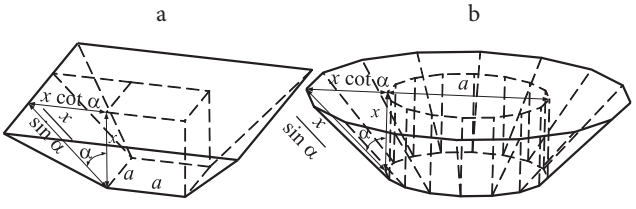

Fig. 4. Diagrams for determination of principle stress action area in the compression zone

Punching force F_u is determined assuming that failure takes place due to cutting the compression zone by the principle stress $\sigma_{1,2}$ in the area A:

$$\min F_u = \sigma_{1,2} A. \quad (10)$$

5. Model verification by experiments

5.1. Method of investigation

Experimental investigations of punching strength for fibre-concrete slab zone around a column are not many. More extensive data of the said investigations are presented by Haralji *et al.* 1995; Swamy, Ali 1982; Urban 1984; Рабинович 2004. Small amount of tests may be explained by great test materials and labour consumption and by complexity.

Thus experimental investigations giving opportunity to assess punching failure character for SFRC slabs more deeply and to verify the theoretical model were performed.

Four RC slabs were produced and tested: three of them were additionally reinforced by steel fibres and one was control slab. Amount of steel fibres was selected as variable in the experiment while concrete class and longitudinal reinforcement were constant values (ρ_l = 1.28 %, Table 2). The experimental slabs were concreted in two series: I series – slabs reinforced by 1% and 1.5% of steel fibres; II series – slabs reinforced by 2% of steel fibres and the control concrete slab.

Cement of Cem 42.5R, sand of (0–4 mm), gravel of (4–16 mm), water and plasticizer were used for the concrete mix. Concrete properties presented in the Table 3. Slab zone at distance of 4d from the column face was additionally reinforced with steel fibres. Steel fibres of "Metalproducts" MPZ50/1 (product No. 1010) with its $\frac{l_f}{d_f} = \frac{50}{1} = 50$, ($f_y$ = 1100 MPa) was used. Three different volume fractions of steel fibres for slabs were applied: 1% – 78.5 kg/m^3, 1.5% – 117.8 kg/m^3, 2% – 157 kg/m^3. They were tested in a special test stand. The slabs are supported on 10 mm thick support along the whole their contour. Cement and sand mix was used to make the supports even. Hydraulic jack of 1000 kN was used for slab loading. Diagram of the test presented in Fig. 5.

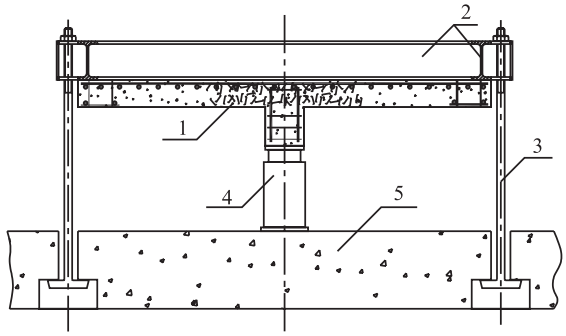

Fig. 5. Slab test diagram: 1 – RC slab; 2 – slab support contour; 3 – steel ties; 4 – hydraulic jack; 5 – force floor

Table 1. Influence of stress diagrams on the angle of the principle stress trajectories

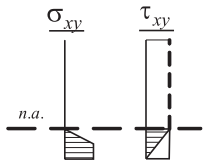	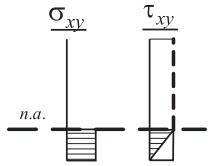	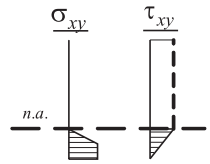	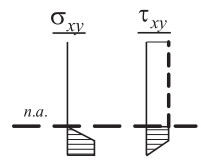
$\omega_\sigma = \frac{(1+\lambda_c)}{2}$	$\omega_\sigma = 1$	$\omega_\sigma = \frac{(1+\lambda_c)}{2}$	$\omega_\sigma = \frac{(1+\lambda_c)}{2}$
$\omega_\tau = 0.5\ldots1$	$\omega_\tau = 0.5\ldots1$	$\omega_\tau = 0.5$	$\omega_\tau = \frac{(2-\lambda_c)}{2}$

ω_τ	α	ω_τ	α	λ_c	α	λ_c	α
0.5	47.27	0.5	57.29	0.5	42.97	0.5	28.64
0.6	42.97	0.6	47.74	0.6	45.83	0.6	32.74
0.7	33.76	0.7	40.69	0.7	48.70	0.7	37.46
0.8	29.54	0.8	35.81	0.8	51.56	0.8	42.97
0.9	26.64	0.9	31.83	0.9	54.43	0.9	49.48
1	23.63	1	28.64	1	57.29	1	57.29

where $tg2\alpha = \frac{2\tau}{\sigma}$; $\sigma = f_c$; $\tau = 0.5 f_c$.

Table 2. Punching carrying capacity results of experimental slabs

Series	Test name	d, m	ρ_l %	V_f, %	$f_{c,\,cube}$, MPa	$F_{sfrc,\,cube}$, MPa	F_{test}, kN	$\frac{F_{test}}{F_{c,cube}}$, 1/m^2
I	FRC-1	0.12	1.28	1	37.54	38.46	417.02	0.0111
	FRC-1.5	0.12	1.28	1.5	37.54	39.60	457.79	0.0121
II	FRC-0	0.12	1.28	0	41.56	–	454.20	0.0109
	FRC-2	0.12	1.28	2	41.56	43.80	519.76	0.0125

Table 3. Concrete strength characteristics

Series	V_f %	$f_{c,\,cube}$, MPa	f_c, MPa	$f_{ct,\,flex}$, MPa	$f_{ct,\,spilt}$, MPa	E_c, MPa
I	0	37.54	30.27	4.41	2.45	32.95
	1	38.46	30.92	5.10	3.13	33.76
	1.5	39.60	31.68	5.75	4.22	34.67
II	0	41.56	33.25	5.13	2.67	35.50
	2	43.80	35.04	7.30	5.23	37.42

Slab deflection at its centre was measured during the test with allowance for movements at corners, longitudinal and transverse (radial) strains of tension and compression zones were measured as well. Slab tension zone strains were measured by mechanical (150 mm base) and by electrical resistance (50 mm base) strain gauges. Mechanical gauges for longitudinal and radial strains were arranged in 3 specific zones: at *d,* 2*d,* 3*d* distances from column face in perpendicular and diagonal directions. Compression slab face stains in *d* zone were measured only by electrical resistance strain gauges. Arrangement of mechanical and electrical resistance strain gauges during the test is presented in Fig. 6.

5.2. Results of experimental investigations

Analysis of available experimental investigation results revealed that steel fibres affect not only the carrying capacity of slabs, plasticity, strains but the failure mode as well. Influence of steel fibres on carrying capacity determined according to the ratio between the actual carrying capacity and the concrete cube strength $\frac{F_{test}}{F_{c,cube}}$. Results of $\frac{F_{test}}{F_{c,cube}}$

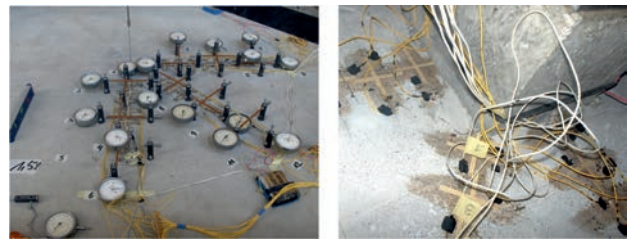

a) in tension zone b) in compression zone

Fig. 6. Arrangement of mechanical and electrical resistance strain gauges

presented in the Table 2 point out that increase in amount of fibres V_f = 1%, 1.5%, 2% resulted in 1.02, 1.09 and 1.15 times greater carrying capacity of slab in comparison with not reinforced one. Similar results were obtained and by other authors (Harajli *et al.* 1995; Kutzing, Konig 2000; Urban 1984).

It was determined by comparison deformation properties of control and SFRC slabs that they differ substantially. For example, slab deflection at its centre at the ultimate load for SFRC slab is 2.8 times (Fig. 7) and at failure – more than 3 times greater than that for the control slab. Moreover, failure modes are very different – the control slab failed suddenly, almost unexpectedly (Fig. 8a) while SFRC slabs failed plastically. When the ultimate load was reached, further loading resulted in decrease of the load carried by the slab and intensive growth of deflections (Fig. 8b). In fact there was no sudden failure.

Analysis of slab deformation during loading and tension zone failure mode revealed evident difference. The first radial crack opened almost at the same load in both slabs: at $0.14F_u$ – in the RC slab without steel fibres and at $0.14F_u$ – $0.17F_u$ – in SFRC slabs. Development of cracks is similar in both radial and tangential directions. For example, all cracks in radial direction at distance d from the column face appeared at $0.1–0.4F_u$, at $2d$ distance – at $0.3–0.6F_u$, while in tangential direction – at $0.25–0.4F_u$ and $0.3–0.6F_u$ respectively. However, cracks in SFRC slabs are distributed much closer to each other. Obvious development of tangential crack width in the zone of $0.5d$ from the column face in the concrete slab is observed when the load is razed from $0.6–1.0F_u$. In SFRC slab it develops at greater distance – $0.7–1.2d$. Distinct formation of the punching cone starts, critical future punching perimeter becomes clearly visible.

These factors altogether show that formation of compression zone depth as well as direction of the main shear stress and its value depends on steel fibres. That is why these factors are assessed in the proposed model.

Saw-cuts of the slabs were made after their tests (Fig. 9). It is seen from the transverse saw-cuts of the slabs that the punching cone in concrete slabs formed at the angle of about 27° ($2d$ from the column face) while in SFRC slabs at smaller angle – 21°–23°(2.4–2.6)d. Diagonal crack develops up to the compression zone which is cut by the principle stress at different angle as well. Moreover, different depth of compression zones is clearly seen. Compression zone depth in SFRC slab is substantially greater than that in common RC slab.

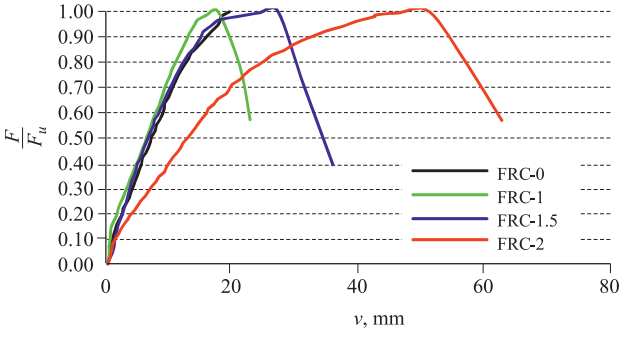

Fig. 7. Load-deflection curves of experimental slabs

6. Analytical model compared with experimental results and models of other authors

Accuracy of proposed model was investigated first. Therefore, comparison of experimental values presented by various authors (Fig. 10) with theoretical values obtained according to the proposed model was made.

Comparison of experimental values presented by various authors with theoretical values according to the proposed model in graphical form is given in Fig. 10 for accuracy assessment of the model for the case with steel fibres. Steel fibres of various geometrical, strength and different anchorage (with full and half bends, wavy and smooth shape) properties were used for comparison as well. It was determined from these data that the average ratio between experimental and theoretical values according to the proposed model $\frac{F_{test}}{F_{calc}} = 1.12$, standard deviation σ_X – 0.08 and coefficient of variation v – 7.0%. According to these statistical data for the proposed model with steel fibres systematic error equals to μ_R = 1.12 and the random one σ_R = 0.08.

Analytical model was compared with different experimental data of other authors (Fig. 10). Specimens of their tests differ by geometrical parameters, concrete strength and longitudinal reinforcement quantity: f_c = 14–120 MPa, f_y = 330–706 MPa, ρ_l = 0.33–3%, d = 99–476 mm.

There are only 11 slab test results (Рабинович 2004 – 4, Urban 1984 – 4, and 3 presented slab tests) for

a) sudden for RC slab b) plastic for SFRC slab

Fig. 8. Failure mode of slabs

a) in RC slab b) in SFRC slab

Fig. 9. Formation of slab punching cone

accurate comparison of model for punching with steel fibres. Even so quite good agreement was obtained and from verification of 11 slabs: average value of ratio $\frac{F_{test}}{F_{calc}} = 1.11$, its standard deviation – 0.21, coefficient of variation – 10.9%. Additional 35 slab tests (Fig. 10) presented for increase in carrying capacity $\frac{F_{test,sfrc}}{F_{test,c}}$, between RC slabs with steel fibres and without it assessment in relation to steel fibre type. Using conditionally equal strength and geometrical characteristics of the slabs (f_c = 30 MPa, f_y = 400 MPa, ρ_l = 1.5%, d = 0.17 mm, dimensions of column are 200×200 mm) verification calculations according to the proposed model in relation to steel fibres type and quantity were performed. After merging together experimental and theoretical comparison of the said 11 and 35 slab results the average value of ratio $\frac{F_{test}}{F_{calc}} = 1.12$, standard deviation and variation coefficient values reduced (0.08 and 6%).

Results obtained according to the proposed model were compared with those obtained according to the models proposed by other authors. Calculations involved 46 versions according to 3 models. Comparison of obtained results is presented in Fig. 11 and their accuracy in the Table 4.

Parallel to *x*-axis regression straights joining related points (Fig. 11) shows that the proposed model is not sensitive to various factors, such as slab geometrical characteristics, steel fibres type, anchorage properties etc. Рабинович (2004) method is very close to the proposed one since it is based on the same design principles of composites, but plastic strains and influence of longitudinal reinforcement on punching strength are not taken into account and larger deviations are obtained. Distinctly stands out Harajli *et al.* (1995) method that demonstrates clearly that not for all cases punching strength analysis using the same empirical relationship for evaluation of steel fibres influence on carrying capacity can be carried out. Results presented in Table 4 shows that proposed model is substantially more accurate than other known models.

Table 4. Experimental results related to theoretical ones for slabs with steel fibres

Author	n	μ_X	σ_X	n
Harajli *et al.* (1995)	11	1.43	0.21	0.15
Рабинович (2004)	11	1.19	0.17	0.14
Proposed model	11	1.11	0.21	0.11
Harajli *et al.* (1995)	46	1.23	0.16	0.13
Рабинович (2004)	46	1.15	0.12	0.11
Suggested model	46	1.12	0.08	0.07

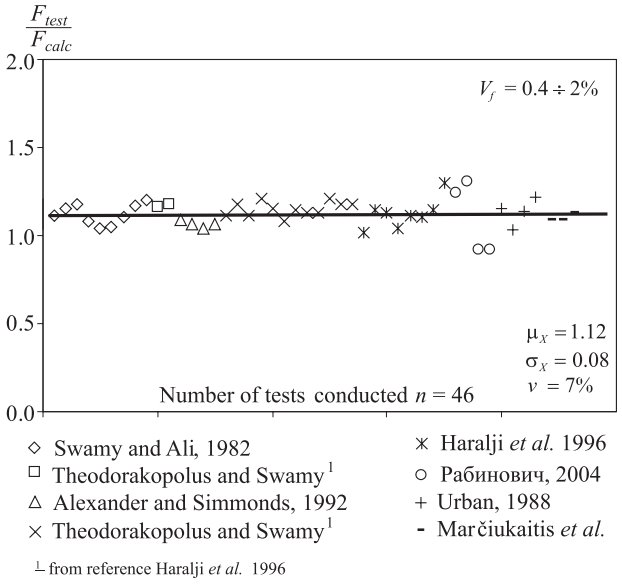

Fig. 10. Accuracy of analytical model with SFRC

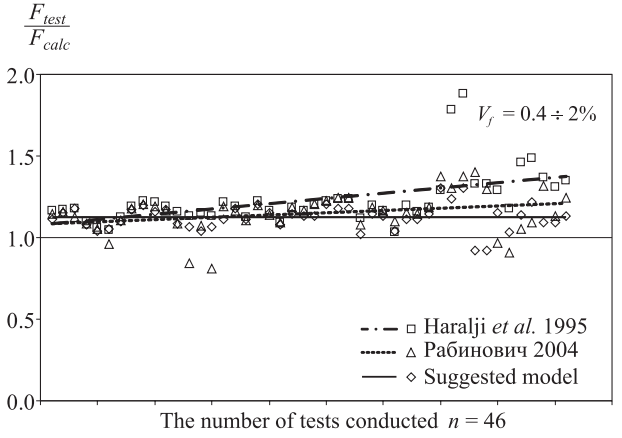

Fig. 11. Comparison of punching with steel fibres analytical model and models of other authors

7. Conclusions

Model for punching strength analysis of bridge flat slab superstructure deck and foundation slab is proposed which allows evaluation of all the most important factors influencing punching strength. It is proven that these factors are concrete strength, amount of longitudinal and steel fibres, and its strength and anchorage properties.

The model gives opportunity to take into account SFRC strength not only in compression zone but also in tension zone as well that is an impossible using model with longitudinal reinforcement only.

Proposed method for evaluation plasticity properties of SFRC and for selection diagrams of normal and tangential stresses acting in slab tension and compression zones during punching and area on which the principle stresses act taking in to account plastic strains of SFRC.

Model accuracy verified comparing with experimental results. Accuracy figures of the proposed model obtained comparing experimental results with analytical ones are: average of the mean values $\mu_x = 1.12$, their square deviations $\sigma_x = 0.08$ and variation coefficient $\nu = 0.07$.

Behaviour under the load of SFRC slabs is substantially different from that of slabs reinforced with steel bars. Their cracking starts at larger loads, spacing of cracks is less, slab failure is of plastic type. At failure slab deflects 3 times more than that without steel fibres.

References

Baikovs, A.; Rocēns, K. 2010. Prediction of the Anticlastic Shape Changes of Hybrid Composite Material, *Journal of Civil Engineering and Management* 16(2): 222–229. doi:10.3846/jcem.2010.25

Broms, C. E. 1990. Punching of Flat Plates – a Question of Concrete Properties in Biaxial Compression and Size Effect, *ACI Structural Journal* 87(3): 292–304.

Choi, K. K.; Park, H. G.; Wight, K. J. 2007. Unified Shear Strength Model for Reinforced Concrete Beams – Part I: Development, *ACI Structural Journal* 104(2): 142–152.

Georgopoulos, T. 1989. Durchstanzlast und Durchstanzwinkel Punkforming Gestutzter Stahlbetonplatten ohne Schubbewehrung [Punching Force and Punching Angle of a Flat Slabs without Shear Reinforcement], *Bauingenieur* [*Civil Engineering*] 64: 187–191.

Hallgren, M. 1996. *Punching Shear Capacity of Reinforced High Strength Concrete Slabs*. PhD thesis. Stockholm: Royal Institute of Technology. 206 p.

Harajli, M. H.; Maalouf, D.; Khatib, H. 1995. Effect of Fibres on the Punching Shear Strength of Slab-Column Connections, *Cement and Concrete Composites* 17(2): 161–170. doi:10.1016/0958-9465(94)00031-S

Kutzing, L.; Koning, G. 2000. Punching Behaviour of High Performance Concrete Columns with Fibre Cocktails, *Lacer* 5: 253–260.

Maalej, M.; Li, V. C. 1994. Flexural/Tensile Strength Ratio in Engineered Cementitious Composite, *Journal of Materials in Civil Engineering* 6(4): 513–528. doi:10.1061/(ASCE)0899-1561(1994)6:4(513)

Menétrey, Ph. 2002. Synthesis of Punching Failure in Reinforced Concrete, *Cement and Concrete Composites* 24(6): 497–507. doi:10.1016/S0958-9465(01)00066-X

Sharma, A. K. 1986. Shear Strength of Steel Fibres Reinforced beams, *ACI Journal Proceedings* 83(4): 624–628.

Shertwood, E. G.; Bentz, E. C.; Collins, M. P. 2007. Effect of Aggregate Size on Beam-Shear Strength of Thick Slabs, *ACI Structural Journal* 104(2): 180–190.

Swamy, R. N.; Ali, S. 1982. Punching Shear Behavior of Reinforced Slab-Column Connections Made with Steel Fiber Concrete, *ACI Journal* 79(5): 392–406.

Szmigiera, E. 2007. Influence of Concrete and Fibre Concrete on the Load-Carrying Capacity and Deformability of Composite Steel-Concrete Columns, *Journal of Civil Engineering and Management* 13(1): 55–61. doi:10.1080/13923730.2007.9636419

Šalna, R.; Marčiukaitis, G. 2007. The Influence of Shear Span Ratio on Load Capacity of Fibre Reinforced Concrete Elements with Various Steel Fibre Volumes, *Journal of Civil Engineering and Management* 13(3): 209–215. doi:10.1080/13923730.2007.9636439

Šalna, R.; Marčiukaitis, G.; Vainiūnas, P. 2004. Estimation of Factors Influencing Punching Shear Strength of RC Floor Slabs, *Journal of Civil Engineering and Management* 10(Suppl 2): 137–142.

Theodorakopoulos, D. D.; Swamy, R. N. 2002. Ultimate Punching Shear Strength Analysis of Slab–Column Connections, *Cement and Concrete Composites* 24(6): 509–521. doi:10.1016/S0958-9465(01)00067-1

Tuchlinski, D. 2004. *Zum Durchstanzen von Flachdecken unter Berücksichtigung der Momenten-Querkraft-Interaktion und der Vorspannung* [Punching of Flat Slabs Considering Moment-Shear Interaction and Prestressing]. PhD. Lehrstuhl und Institut für Massivbau, RWTH Aachen, 2005. 149 p.

Urban, T. 1984. Badania żelbetowych złączy płytowo-słupowych z dodatkiem drutu ciętego w strefie przysłupowej [Tests of Reinforced Concrete Slab-Pole Connectors with Wire Cut in the Punching Zone], *Inżineria i Budownictwo* [*Engineering and Constructions*] 10: 390–393.

Zink, M. 1999. *Zum Biegeschubversagen schlanker bauteile aus hochleistungsbeton mit und ohne schubbewehrung* [Bending to Shear Failure of Slender Components of High Performance Concrete with and Without Shear Reinforcement]. PhD. Universitat Leipcig. 172 p.

Рабинович, Ф. Н. 2004. *Композиты на основе дисперсно-армированных бетонов. Вопросы теории и проектирования, технология, конструкции:* Монография. [Rabinovic, F. N. Composite Structures, Based on Fibre Reinforcement. The Questions of Theory, Design, Technology and Structures]. Москва: АСВ. 506 с.

Received 11 October 2010; accepted 20 May 2011